NUCLEAR THEORY, Vol. 33 (2014)
eds. A.I. Georgieva, N. Minkov, Heron Press, Sofia

Proton Form Factors in Space-like and Time-Like Regions

E. Tomasi-Gustafsson[1], **S. Pacetti**[2], **R. Baldini-Ferroli**[3]

[1]CEA, IRFU, SPhN, Saclay, 91191 Gif-sur-Yvette Cedex, France and CNRS/IN2P3, Institut de Physique Nucléaire, UMR 8608, 91406 Orsay, France
[2]Dipartimento di Fisica and INFN Sezione di Perugia, 06123 Perugia, Italy
[3]INFN, Laboratori Nazionali di Frascati, 00044 Frascati, Italy

Abstract.

Electromagnetic proton form factors are reviewed, and the experimental results are presented and compared to available theoretical models. Future perspectives at different facilities using elastic electron proton scattering in the space-like region and the annihilation reactions $\bar{p}+p \leftrightarrow e^{+}+e^{-}$ in the time-like region are summarized. Based on the existing data, the necessity for a global description of form factors in the full kinematical region is stressed. We describe an attempt of a physical interpretation of form factors in space-like and time-like regions.

1 Introduction

Electromagnetic form factors (FFs) are fundamental quantities, which describe the internal structure of hadrons and the dynamic behavior of their charge and magnetic distributions. They are traditionally measured through elastic electron-proton (ep) scattering assuming the exchange of a virtual photon of squared momentum q^2, which is here space-like (SL). Polarization phenomena were studied and developed by the Kharkov school since the mid of last century, see Refs. [1, 2] and references therein. Whereas the unpolarized cross section contains only the (modulus squared of) FFs, polarization observables contain the interference of the amplitudes, giving access to the sign of FFs in SL region.

Although experiments and theories have been developed since decades, recently the opening of new experimental possibilities has driven an intensive and renewed activity in the field.

The precise data which have been obtained, mostly at the Jefferson Laboratory (JLab), have shown that the behavior of the electric and magnetic distributions inside the proton are different (Ref. [3] and references therein), contrary to what was previously assumed, and that the neutron electric FF is small, but does not vanish. In particular the electric proton FF does not follow a dipole distribution, and might even cross zero and becomes negative at large momentum transfer. This issue will be further investigated after the upgrade of JLab, where experiments are foreseen for all four nucleon FFs: electric and magnetic, for proton and neutron, in the three Halls: A, B, and C at 11 GeV maximum energy.

At electron-positron facilities the quasi real electron method, called initial state radiation (ISR), has been successfully applied by the BABAR collaboration at SLAC, allowing to measure FFs in a wide time-like kinematical region (Ref. [4] and references therein). Moreover, the BESIII collaboration at BEPCII [5] will measure very precisely proton and neutron FFs in the threshold region [6]. In next future an antiproton beam with momentum up to 15 GeV will be available at FAIR (Darmstadt) [8] and measurements by the PANDA collaboration should allow firstly the individual measurement of electric and magnetic FFs in the time-like region at relatively high momentum transfer [7].

From the theoretical point of view, any model which describes the properties of hadrons, should reproduce static properties as masses and magnetic moments as well as dynamical properties induced by the inner complex structure of the constituents. Form factors are a very convenient playground for testing the validity of theory on experimental data: they enter in the most general expression for the electromagnetic hadronic current and they are directly measurable through differential cross section and polarization observables, in ep elastic scattering and in the annihilation reactions $e^+ + e^- \leftrightarrow \bar{p} + p$ for time-like (TL) values of the momentum transfer squared.

Presently, FFs are not directly calculable from QCD. There are different models which give a satisfactory, but partial description of the nucleon properties. In particular, most of the models were developed for describing data in the SL region. Classes of models as those based on dispersion relations and vector dominance may be constructed with the necessary properties to be extended to the whole kinematical region.

This contribution is based on an extended review by the authors [9].

2 The Space-Like Region

Since the pioneering experiments of Hofstadter [10], several measurements of the unpolarized cross section for ep elastic scattering have been performed, at larger and larger $Q^2 = -q^2$ values and with better precision. Single arm experiments, where only the lepton is (magnetically) analyzed, are in principle sufficient. In practice, coincidence experiments with the detection of both scattered electron and proton are necessary to reduce the background. However, experiments wiht precise determination of the four momenta of both particles have not yet been reported. From unpolarized cross section measurements the determination of G_E and G_M has been done up to $Q^2 \simeq 8.8$ GeV^2 [11] and G_M has been extracted up to $Q^2 \simeq 31$ GeV^2 [12] under the assumption that the electric FF vanishes ($G_E = 0$) or that it equals the magnetic FF, G_M, scaled by the proton magnetic moment $G_E = G_M/\mu_p$ (Figure 1).

Note that each experiment differs for the radiative corrections which have to be applied. Typically, first order radiative corrections can reach up to 50%

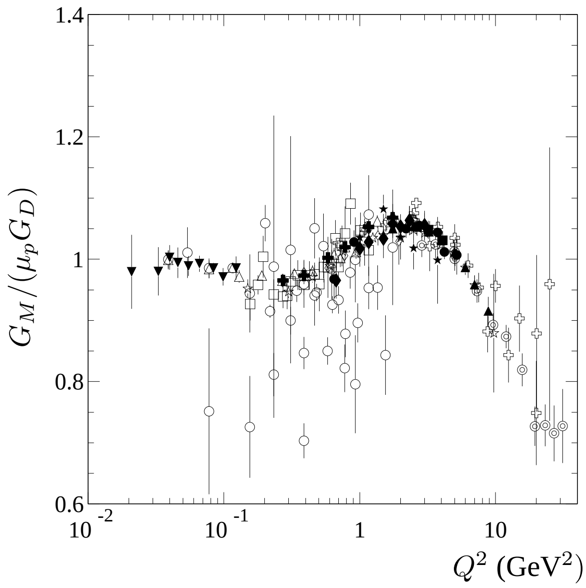

Figure 1. World data on $G_M/\mu_p G_D$ as a function of Q^2.

on the unpolarized cross section at large Q^2, whereas they cancel (at least those which factorise out) in the polarization ratio. This technique, which requires a longitudinally polarized electron beam and the measurement of the transverse over longitudinal polarization of the scattered proton in the reaction plane was used by the JLab GEp collaboration in a series of experiments, measuring precisely the ratio of the electric to magnetic FFs up to Q^2 =8.9 GeV^2 [3]. The measurement of the FFs ratio is expected to give very precise results, because, at first order, the beam helicity as well as the analyzing power of the proton polarimeter cancels, reducing the systematic errors and being more sensitive to a small contribution of the electric FF. Moreover, the experiment showed a surprising behavior: a monotone decreasing of the ratio when Q^2 increases. An extrapolation of this tendency at large Q^2 may lead to the ratio passing through zero and even becoming negative. As G_M is supposed to be well known from the unpolarized cross section (as the magnetic term dominates at large Q^2), the present understanding is that G_M follows a dipole (Q^{-4}) behavior and that the electric FF follows a a steeper decreasing behavior, see Figure 2a.

However, the ratio $\mu_p G_E/G_M$ from unpolarized measurements shows a behavior consistent with unity, with a larger error as Q^2 increases, Figure 2a. The reason has to be likely attributed to the contribution of higher order radiative corrections. Note that unpolarized data, selected in experiments where radiative corrections did not exceed 20% also show a deviation of the ratio from unity (Figure 2b).

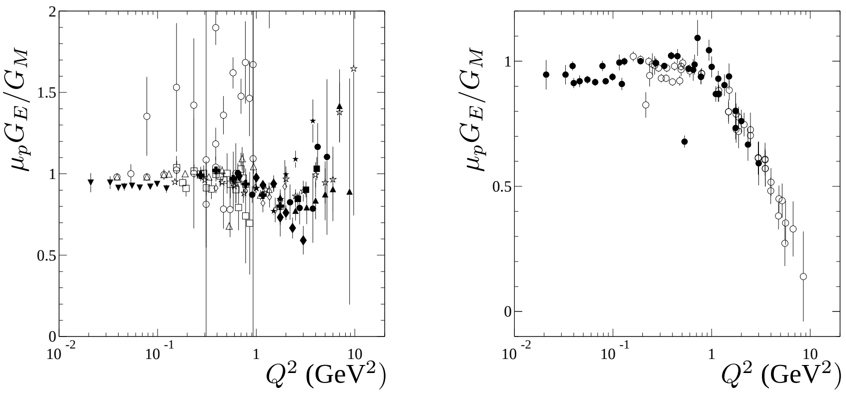

Figure 2. a) World data on $\mu_p G_E/G_M$ as a function of Q^2 from unpolarized ep elastic scattering, b) Ratio $\mu_p G_E/G_M$ from polarization data (open symbols) and from selected unpolarized cross section data (solid symbols).

3 The Time-Like Region

In the TL region, the differential cross section contains the full information on the reaction mechanism and on FFs. The expression of the differential cross section for $\bar{p} + p \to e^+ + e^-$ is [13]

$$\frac{d\sigma}{d\cos\theta} = \frac{\pi\alpha^2}{2\beta q^2}\Big[(1+\cos^2\theta)|G_M|^2 + \frac{1}{\tau}\sin^2\theta|G_E|^2\Big];\ \beta = \sqrt{1 - \frac{4M^2}{q^2}}, \quad (1)$$

M is the proton mass and θ is the center of mass electron emission angle. The individual determination of the FFs in the TL region has not yet been done due to the limitation in the intensity of antiproton beams or the luminosity of e^+e^- colliders, which did not allow a precise and complete measurement of the angular distribution of the outgoing leptons.

The results are often given in terms of an effective FF derived from the total (or integrated) cross section of the reaction $e^+ + e^- \leftrightarrow \bar{p} + p$ under the assumption $G_E = G_M$:

$$G_{\text{eff}} = \sqrt{\frac{|G_E|^2 + 2\tau\,|G_M|^2}{1 + 2\tau}}\,. \quad (2)$$

or the equivalent form in case of limited angular range.

At the moment the best data have been obtained by BABAR [4], see Figure 3. The main features of these data are a clear step at threshold, a steep decreasing of the effective FF, followed by a rather flat cross section in a ~ 200 MeV energy range. Several structures appear, on a general trend which follows

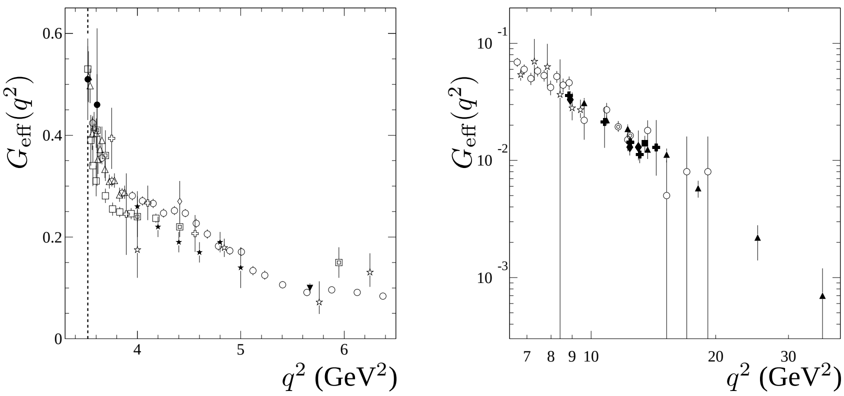

Figure 3. World data of the effective proton FF, $G_{\rm eff}(q^2)$, as a function of the squared-momentum transfer, in the low (left) and high (right) momentum transfer regions.

the dipole behavior. The data, reaching $q^2 \sim 35$ GeV^2, have been obtained using the process $e^+ + e^- \to \bar{p} + p + \gamma$ (ISR) where, in the case when the electron remains on shell after the photon emission, the cross section can be factorized in a term which depends on the energy and angle of the (hard) photon and in the cross section for the process of interest $e^+ + e^- \to \bar{p} + p$.

Let us note other interesting aspects:

- the threshold region is particularly intriguing. It has been observed that the the presence of the Coulomb factor plays a specific role compensating the phase-space relative velocity. This induces a non vanishing cross section just above threshold, and the extrapolation of the flat cross section up to the threshold gives:

$$\sigma(e^+e^- \to \overline{p}p)(4M^2) = (0.85\,\mathrm{nb})\,|G(4M^2)|^2\,, \tag{3}$$

  where $G(4M_p^2)$ is the common value of the electric and magnetic FF at threshold. The identity of Eq. (3) compared to the data, implies the rather peculiar result that $|G(4M_p^2)| = |G_E(4M_p^2)| = |G_M(4M_p^2)| = 1.00 \pm 0.05$, like in the case of a pointlike fermion [14].

- At low momentum transfer, in SL region, the possibility to extract FFs with improved precision allows to get a better determination of the proton radius and to reduce the error on the extraction of strange and axial FFs,

- At large momentum transfer, analytical properties of FFs impose constrains that should be experimentally verified. The hermiticity of the current operator implies that FFs are real in the SL region, and fulfil the Schwarz reflection principle in the TL region, where they are complex. Following the Phragmèn-Lindelöf (P-L) theorem, since in the SL region

FFs are real, the TL limit at infinite q^2 has to be real. In other words, as $q^2 \to \infty$, the imaginary part of $G_M(q^2)$ vanishes faster than the real part. It implies that the phase goes to an integer multiple of 2π radians. This result holds for each FF.

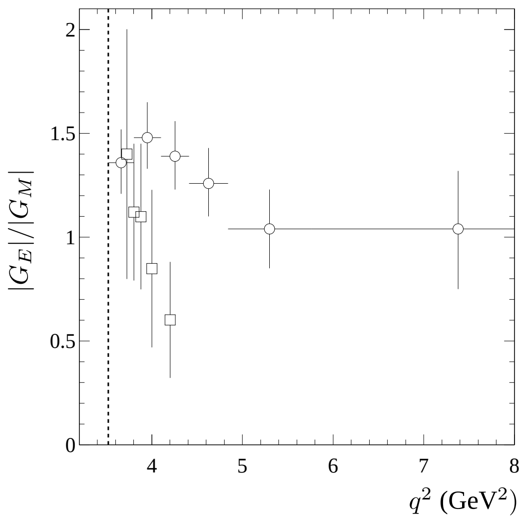

Figure 4. Modulus of the ratio G_E/G_M in the TL region. The data are from: Ref. [4] (open circles) and Ref. [15] (open squares). The vertical dashed line in the left panel shows the production threshold $q^2 = 4M^2$.

4 Phenomenological Models

Several models have been developed to describe hadron FFs. Let us note that mesons and baryons seem to be different objects, and it is not straightforward to extrapolate to baryons the models which have been built for mesons. The study of FFs is especially interesting in the intermediate energy region, where the perturbative description of the nucleon in terms of three quarks does not hold and effective degrees of freedom have to be introduced.

Perturbative Quantum Chromodynamics gives predictions on the asymptotic behavior of FFs, but the experiments have to define the kinematical region of applicability. Vector Meson Dominance models assume that a photon interacts with the nucleon through a vector meson, which has the same quantum numbers. The success of this approach is due to the fact that they can be extended to many meson resonances. A limited number of parameters with physical meaning as masses and coupling constants allows to reproduce the data. Chiral Perturbation Theory has brought deep insight on the nucleon structure, in particular at low Q^2. Soliton models and Conformal Field Theories have been recently applied to the TL region. Other phenomenological concepts have been developed during the recent years and applied to FF data, trying in particular to reproduce the decrease of the FF ratio: cloudy bag and diquark, quark-hadron duality, generalized parton distributions...(for a review see Ref. [9]).

Let us stress that not all the nucleon models reproduce equally well all four (proton, neutron, electric and magnetic) nucleon FFS and have the necessary analytical properties to be applied in both regions, of positive and negative q^2. In Ref. [17] a study of the classes of models which can be analytically continued in the TL region, together with a global fit to the available SL and TL data, was performed, selecting those models which may be applied both in scattering and annihilation regions.

Recently a model was suggested to interpret nucleon electromagnetic form factors both in space and TL regions [18]. It assumes that in ep elastic scattering and in the $e^+e^- \leftrightarrow \bar{p}+p$ annihilation a large quantity of energy (mass) and momentum is concentrated in a small volume creating a strong gluonic field, i.e., a gluonic condensate of clusters with a randomly oriented chromo-magnetic field. This condition generates an effect similar to the screening of a charge in plasma. In the region of strong chromo-magnetic field the color quantum number of quarks does not play any role, due to stochastic averaging. When the color quantum number of quarks of the same flavor vanishes, then, due to Pauli principle, identical quarks (uu for proton or dd for neutrons) are pushed outside the internal region of the proton (or the neutron). The third quark is attracted by one of the identical quarks and forms a compact diquark. In the regions where the gluonic field is weaker the color state of quarks is restored. The creation of a quark-diquark dipole system occurs when the attraction force exceeds the stochastic force of the gluon field. These considerations apply to the scalar part of the field, and explain the additional suppression of the electric FF, leaving unchanged the predictions from quark counting rules for the magnetic FF. Quark counting rules apply to the vector part of the interaction, and are derived from the interaction of the virtual photon with three independent quarks.

Similarly, in TL region, above the physical threshold, $q^2 \geq 4M^2$, the vacuum state created at the collision transfers all the energy to a S-wave state with total spin 1, consisting in at least six massless valence quarks, a set of gluons and a sea of current $q\bar{q}$ quarks, with total energy $q_0 > 2M$, and total angular momentum unity. At this point the system is a pair of (colorless) proton and antiproton each formed by three bare quarks (antiquarks). The quarks as partons have no structure: the Pauli FF vanishes and the Dirac FF is unity ($|G_E| = |G_M| = 1$), which may explain the point-like behavior of FFs at threshold. The anomalous magnetic moment appears when the system starts to expand and to cool down. The current quarks (antiquarks) absorb gluons and transform into constituent quarks (antiquarks).

The neutral plasma acts on the distribution of the electric charge (not of the magnetic charge) as an additional suppression factor. Similarly and for the same reasons as in SL region, also in TL region an additional suppression of the electric FF is expected.

The definition of FFs can be generalized to

$$F(q^2) = \int_{\mathcal{D}} d^4x e^{iq_\mu x^\mu} \rho(x),\ q_\mu x^\mu = q_0 t - \vec{q}\cdot\vec{x} \tag{4}$$

where $\rho(x) = \rho(\vec{x}, t)$ is the space-time distribution of the electric charge in a space-time volume $\mathcal{D}$. In the scattering channel and in the Breit frame, the usual definition of FFs is recovered:

$$F(q^2) = \delta(q_0) F(Q^2),\ Q^2 = -(q_0^2 - \vec{q}^2) > 0, \tag{5}$$

where zero energy transfer is implied.

In the annihilation channel, in the center of mass reference frame where the three-dimensional transferred momentum vanishes, $q_0 = \sqrt{q^2}$, and we have:

$$F(q^2) = \int_{\mathcal{D}} dt e^{i\sqrt{q^2}t} \int d^3\vec{r} \rho(\vec{r}, t) = \int_{\mathcal{D}} dt e^{i\sqrt{q^2}t} \mathcal{Q}(t), \tag{6}$$

where $\mathcal{Q}(t)$ is a scalar quantity which can be interpreted as the time evolution of the charge distribution in the physical domain $\mathcal{D}$.

This model has one free parameter, in principle calulable, and it is expected to work from moderate values of the momentum transfer. It gives a good description of the GEp data, and of G_M, where it overlaps with the dipole predictions.

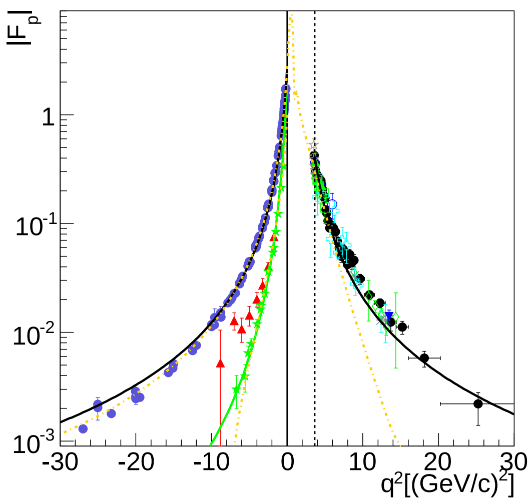

Figure 5. World data on proton FFs as function of q^2. **Space-like region:** G_M data (blue circles), electric FF, G_E, from unpolarized measurements (red triangles) and from polarization measurements (green stars). The solid, green (black) line is the model prediction of Ref. [18] for $G_E(G_M)$. **Time-like region:** $|G_E| = |G_M|$ world data for $q^2 > 4M^2$ and model prediction (black,solid line) from the dipole function. The orange,dash-dotted line is the prediction from [19].

The results are illustrated in Figure 5, compared to the data and to the model of Ref. [19].

5 Conclusion

The present status on electromagnetic FFs has been illustrated in SL and TL regions. After several decades of measurements and theoretical studies, open questions remain to be investigated with ongoing and future experiments, and a satisfactory theory which gives a quantitative description of the nucleon dynamical internal structure in all the kinematical range is not yet available.

The proton SL FFs are twice smaller than the corresponding FFs in TL region. An enhancement of α_s, can be obtained in principle in the analytical continuation to the TL region, by introducing phenomenological soft contributions, which contain Sudakov double logarithms. However, it was concluded in Ref. [16], that perturbative QCD can not give such large enhancement.

For the neutron TL FF, the four points measured at FENICE, if confirmed, are twice as large as the proton TL FF at the mirror q^2 value.

Advances are expected in next future: in SL region Mami-Mainz will continue the programme of precise FFs measurements at low Q^2, on proton , neutron, and deuteron. At JLab, experimental programs on all four nucleon FFs with the high quality (polarized) electron beams are planned.

In TL region, the threshold region will be further investigated. A measurement of the ratio $|G_E|/|G_M|$ at a few percent level will be achieved by BESIII, but mostly below 3 GeV in the center of mass. CMD3 and SND at VEPP2000 may give an answer on the question of the possible presence of $D-$wave close to the threshold. The ISR method can be used, but unfortunately, in the case of BESIII, the BEPCII collider foreseen integrated luminosity will probably not reach the one obtained by BABAR, even if there is a gain of at least a factor of ten, collecting data at lower center-of-mass energies. Only the advent of the future B or τ/charm factories will give an answer to the question of the $\bar{p}p$ cross section at threshold.

PANDA will be able to measure the annihilation cross section up to large values of momentum transfer and to determine the individual value of the electric and magnetic FFs at moderate q^2. Dispersion relation approaches may give a reliable description but they require the knowledge of the individual FFs, in the the whole domain, in particular in the unphysical region where resonances are expected to strongly contribute. Note that this region can be accessed through the reaction $\bar{p}+p \to e^+ + e^- + \pi^0$, assuming $t(u)$ channel exchange [20].

Acknowledgements

This work was partially supported by the Italian INFN and the Physics Department of the Perugia University, as well as the French GDR-PH-QCD and the PICS-IN2P3 grant n. 5895.

References

[1] A. Akhiezer, M. Rekalo, *Sov. Phys. Dokl.* **13** (1968) 572.
[2] A. Akhiezer, M. Rekalo, *Sov. J. Part. Nucl.* **4** (1974) 277.
[3] A. Puckett, et al., *Phys. Rev. Lett.* **104** (2010) 242301.
[4] J. Lees, et al., *Phys. Rev.* **D87** (2013) 092005.
[5] *Beijing Electron Positron Collider*, URL: `http://www.ihep.ac.cn/english/E-Bepc`
[6] *BESIII Experiment*, URL: `http://bes3.ihep.ac.cn`
[7] *The PANDA Experiment website*, URL: `http://www-panda.gsi.de`
[8] *The new large scale accelerator facility in Europe*, URL: `http://www.fair-center.eu`
[9] S. Pacetti, R. Baldini-Ferroli and E. Tomasi-Gustafsson, to be published in *Physics Reports*.
[10] R. Hofstadter, F. Bumiller, M. Croissiaux, *Phys. Rev. Lett.* **5** (1960) 263-265.
[11] L. Andivahis, et al., *Phys. Rev.* **D50** (1994) 5491-5517.
[12] R. Arnold, et al., *Phys. Rev. Lett.* **57** (1986) 174.
[13] A. Zichichi, S. Berman, N. Cabibbo, R. Gatto, *Nuovo Cim.* **24** (1962) 170-180.
[14] R. Baldini, S. Pacetti, A. Zallo, A. Zichichi, *Eur. Phys. J.* **A39** (2009) 315-321.
[15] G. Bardin, et al., *Nucl. Phys.* **B411** (1994) 3-32.
[16] A. Bakulev, A. Radyushkin, N. Stefanis, *Phys. Rev.* **D62** (2000) 113001.
[17] E. Tomasi-Gustafsson, F. Lacroix, C. Duterte, G. Gakh, *Eur. Phys. J.* **A24** (2005) 419-430.
[18] E. Kuraev, E. Tomasi-Gustafsson, A. Dbeyssi, *Phys. Lett.* **B712** (2012) 240-244.
[19] F. Iachello, Q. Wan, *Phys. Rev.* **C69** (2004) 055204.
[20] C. Adamuscin, E.A. Kuraev, E. Tomasi-Gustafsson, F.Maas, *Phys. Rev.* **C75** (2004) 045205.